PRP Pharmacology Research & Perspectives
Open Access

ORIGINAL ARTICLE

# Pharmacological evaluation of a series of smoothened antagonists in signaling pathways and after topical application in a depilated mouse model

Emilie Lauressergues[1,*], Peter Heusler[1,*], Fabrice Lestienne[1], David Troulier[2], Isabelle Rauly-Lestienne[1], Amélie Tourette[1], Marie-Christine Ailhaud[1], Claudie Cathala[1], Stéphanie Tardif[1], Delphine Denais-Lalième[3], Marie-Thérèse Calmettes[3], Anne-Dominique Degryse[3], Antoine Dumoulin[2], Luc De Vries[1] & Didier Cussac[1]

[1]Department of Cellular and Molecular Biology, Pierre Fabre Research Centre, 17, avenue Jean Moulin, F-81106 Castres Cedex, France
[2]Department of Developability, Pierre Fabre Research Centre, Castres, France
[3]Laboratory Animal Resources, Pierre Fabre Research Centre, Castres, France

**Keywords**
basal cell carcinoma, Hedgehog pathway, smoothened inhibitor, smoothened receptor, sonidegib, topical application, vismodegib

**Correspondence**
Didier Cussac, Department of Cellular and Molecular Biology, Centre de Recherche Pierre Fabre, 17, avenue Jean Moulin, F-81106 Castres Cedex, France.
Tel: +33-5 63 71 43 62;
Fax: +33-5 63 71 43 63;
E-mail: didier.cussac@pierre-fabre.com

**Funding Information**
No funding information provided.

Received: 31 July 2015; Revised: 15 December 2015; Accepted: 20 December 2015

***Pharma Res Per 4(2), 2016, e00214, doi: 10.1002/prp2.214***

doi: 10.1002/prp2.214

*These two authors contributed equally to this work.

## Abstract

The Hedgehog (HH) pathway has been linked to the formation of basal cell carcinoma (BCC), medulloblastoma, and other cancers. The recently approved orally active drugs vismodegib (GDC-0449) and sonidegib (LDE–225) were not only efficacious for the treatment of advanced or metastatic BCC by antagonizing the smoothened (SMO) receptor, but also produced important side effects, limiting their use for less invasive BCC. Herein, we compared a large series of SMO antagonists, including GDC-0449 and LDE-225, the clinically tested BMS-833923, CUR-61414, cyclopamine, IPI-926 (saridegib), itraconazole, LEQ-506, LY-2940680 (taladegib), PF-04449913 (glasdegib), and TAK-441 as well as preclinical candidates (PF-5274857, MRT-83) in two SMO-dependent cellular assays and for G-protein activation. We report marked differences in inhibitor potencies between compounds as well as a notable disparity between the G-protein assay and the cellular tests, suggesting that classification of drugs is assay dependent. Furthermore, we explored topical efficacies of SMO antagonists on depilated mice using Gli1 and Ptch1 mRNA quantification in skin as biomarkers of the HH signaling inhibition. This topical model rapidly discriminated drugs in terms of efficacies and potencies for inhibition of both biomarkers. SMO antagonists showed also a large variation in their blood and skin partition, suggesting that some drugs are more favorable for topical application. Overall, our data suggested that in vitro and in vivo efficacious drugs such as LEQ-506 and TAK-441 may be of interest for topical treatment of less invasive BCC with minimal side effects.

## Abbreviations

BCC, basal cell carcinoma; CGNP, cerebellar granule neuron precursor; CHO, Chinese hamster ovary; DMSO, dimethyl sulfoxide; EtOH, ethanol; GLI, glioma-associated oncogene homolog; HH, Hedgehog; IHC, immunohistochemistry; MEM, minimum essential medium; PBS, phosphate-buffered saline; PCR, polymerase chain reaction; PG, propylene glycol; PTCH, patched; qPCR, quantitative polymerase chain reaction; RT-PCR, real-time polymerase chain reaction; SHH, sonic Hedgehog; SMO, smoothened receptor.

## Introduction

Smoothened (SMO) is a G-protein-coupled receptor (GPCR) that plays a pivotal role within the Hedgehog (HH) signaling pathway. Initially described in *Drosophila*, this pathway is mainly implicated in developmental processes, but regulates homeostasis in adult organisms as well (Varjosalo and Taipale 2008). The HH signaling cascade is initiated by binding of secreted Hedgehog ligands (three of which have been identified in mammals) to the transmembrane receptor patched (PTCH), leading to a relief of the constitutive PTCH-dependent repression of the SMO coreceptor. Downstream events mediated by SMO activation are complex and often depend on the interactions with other pathways (Ruat et al. 2014), but in the paradigmatic "canonical" pathway implicate modifications of transcriptional activity via activation of the glioma-associated oncogene homolog (GLI) transcription factors (Scales and de Sauvage 2009; Teperino et al. 2014).

Abnormal activation of the HH pathway (often due to PTCH or SMO receptor mutations) has been linked to several cancers, in particular to basal cell carcinoma (BCC), medulloblastoma, and rhabdomyosarcoma (Varjosalo and Taipale 2008; Mas and Altaba 2010; Ng and Curran 2011; Amakye et al. 2013; Xie et al. 2013). Accordingly, attenuating the HH pathway at the level of SMO via small molecule inhibitors represents a promising approach for cancer therapy (Mas and Altaba 2010; Amakye et al. 2013; Ruch and Kim 2013). Consistent with this, two recently developed drugs targeting the SMO receptor, vismodegib (GDC-0449) and sonidegib (LDE-225; erismodegib), have obtained approval for oral treatment of locally advanced and metastatic BCC not illegible to either surgery or radiotherapy. These drugs are now followed by numerous other SMO inhibitors under preclinical or clinical investigation for BCC or other types of cancer (Peukert and Miller-Moslin 2010; Lin and Matsui 2012; Dreier et al. 2014).

A major drawback of systemic blockade of the HH pathway is the associated induction of severe side effects such as muscle spasms, dysgeusia, alopecia, weight loss, and fatigue, leading to a high rate of treatment discontinuation (Siu et al. 2010; Sekulic et al. 2012; Dreier et al. 2014; Rodon et al. 2014). This type of blockade also precludes their use for superficial non-invasive BCC, which represents the majority of skin lesions. An interesting alternative approach to minimize or avoid these side effects could be a topical application of HH-targeting drugs. Indeed, topical application of the SMO antagonists CUR-61414, cyclopamine, or LDE-225 has been investigated in the clinic on human BCC (Tas and Avci 2004; Skvara et al. 2011; Tang et al. 2011). While CUR-61414 was ineffective, cyclopamine and LDE-225 promoted a significant reduction in BCC size, although their development in this indication has been stopped essentially because of the poor developability in the case of cyclopamine and for a repositioning to other indications in the case of LDE-225. Nevertheless, the encouraging results obtained with LDE-225 in a few patients and the arrival of several new SMO antagonists at different stages of development present an incentive to test and compare their potential use as a topical formulation for BCC treatment.

Surprisingly, in spite of the active research in this area, there are few and rather restricted comparative studies on the efficacy of diverse SMO inhibitors in preclinical models of SMO activity. In order to contribute to such a comparison, we present here our results obtained with GDC-0449 and LDE-225 and with a large series of SMO antagonists that are in preclinical development (PF-527857, MRT83) or have already been tested in (ongoing or discontinued) clinical trials (BMS-833923, CUR-61414, IPI-926, itraconazole, LEQ-506, LY-2940680, PF-04449913, TAK-441) for BCC and other types of cancers. These compounds were tested in four early screening assays on SMO activity. First, the compounds were characterized in three different in vitro assays for their basic SMO inhibitory properties by measuring SMO-mediated G-protein activation (Riobo et al. 2006), SHH-induced proliferation of granule cell precursor cells (Pons et al. 2001), and GLI1 mRNA induction by SHH in DAOY cells (Bar et al. 2007). In a second step, we specifically addressed the topical efficiency of SMO antagonists using a depilated mouse model implicating an overinduced HH pathway. This preclinical model has already been used to evaluate the efficacies of LDE-225 and CUR-61414 after several topical applications through the inhibition of Gli1 and Ptch1 expression, both biomarkers of HH pathway activity (Skvara et al. 2011; Tang et al. 2011). We extended the studies in this model to compare the efficiency of a large series of SMO antagonists for inhibition of Gli1 and Ptch1 expression after a single topical application, a more challenging approach which might be more predictive for the efficacy of topical BCC treatment. At the same time, drug partitioning between blood and skin was examined in order to identify drugs with a preferential skin tropism and low systemic circulation, to minimize side effects associated with systemic delivery of SMO antagonists.

## Materials and Methods

### [$^{35}$S]GTP$\gamma$S incorporation experiments

Membranes were prepared from CHO-K1 cells stably or transiently expressing recombinant wild-type (wt) human

smoothened receptors (SMO) or transiently expressing mutant SMO M2 (SMO W535L) or SMO D473H variants. Receptor-mediated G-protein activation was determined by measuring [$^{35}$S]GTP$\gamma$S (1250 Ci/mmole; NEN, PerkinElmer, France) incorporation. Briefly, membranes were preincubated 30 min at 30°C with receptor ligands in a buffer containing 20 mM HEPES, pH 7.4, 3 $\mu$M GDP, 3 mM $MgCl_2$, 100 mM NaCl. The reaction was started by the addition of 0.5 nM [$^{35}$S]GTP$\gamma$S in a final volume of 500 $\mu$L in 96-well plates and incubation was performed for an additional 30 min. Experiments were terminated by rapid filtration through Unifilter-96 GF/B filters (PerkinElmer Life Sciences, Boston, MA, USA) using a Filtermate harvester (PerkinElmer Life Sciences). Radioactivity retained on the filters was determined by liquid scintillation counting using a TopCount microplate counter (PerkinElmer Life Sciences). Inhibition of constitutive receptor activity was determined relative to the effect induced by the reference antagonist, cyclopamine. Basal binding was therefore defined as 0 %, whereas the effect of cyclopamine (10 $\mu$M) on basal [$^{35}$S]GTP$\gamma$S incorporation was defined as full inverse agonism (−100%).

## SHH-induced GLI1 mRNA expression in DAOY cells

DAOY cells (Ref HTB-186, ATCC, Manassas, VA, USA) were serum starved 16 h before experiments and subsequently incubated for 24 h with SHH (50 nM) and the studied compounds at different concentrations. Cells were then washed twice with PBS and stored at −80°C until RNA isolation. Total RNA was isolated using the RNeasy Mini Kit on a QIAcube automation system (Qiagen, CA, USA). The amount and quality of extracted RNA were determined using the 2100 Bioanalyzer (Agilent Technologies, Santa Clara, CA, USA). For reverse transcription, 500 ng of total RNA was used to generate cDNA by using a QuantitecReverseTranscription Kit (Qiagen, CA, USA) in a total volume of 20 $\mu$L. An internal step to eliminate genomic DNA contamination was included. Real-time PCR was carried out on the CFX96 Real-Time PCR Detection System (Bio-Rad) using gene-specific primers and SsoFast EvaGreen supermix (Bio-Rad Laboratories, Richmond, CA, USA). Primer sequences are given separately in the Supporting Information. PCR reactions were performed as duplicates in a final volume of 15 $\mu$L as follows: 45 sec at 98°C to activate "hot start" enzyme and 40 cycles at 95°C for 2 sec, 62°C for 5 sec, followed by a fusion curve from 70°C to 90°C (0.5°c every 5 sec) to determinate the specific $T_m$ of each amplicon. This protocol allowed us to obtain a qRT-PCR efficacy >95%.

## Data analysis

After a prior analysis of housekeeping genes using the NormFinder algorithm (Andersen et al. 2004) to determine the most appropriate normalization tool, human GAPDH, human RPLP0, and human YWHAZ were used as internal reference. A geometric mean of Ct values of these three genes was used to normalize the GLI1 Ct value for each sample with the following formula (Vandesompele et al. 2002): Relative Expression = $2^{-\mathrm{GLI1Ct}}/2^{-\mathrm{GeoMeanGN}}$. In pharmacological evaluations, stimulation by SHH at 50 nM was defined as 100 % value.

## Proliferation of cerebellar granule cells

Cerebella from OFA rats at postnatal day 8 were dissected in a neurobasal medium supplemented with B27 and penicillin–streptomycin. Pooled cerebella (four cerebella for 9 mL medium) were digested for 30 min at 37°C with 250 $\mu$g/mL trypsin dissolved in dissection buffer. Digestion was stopped by addition of buffer containing 250 $\mu$g/mL trypsin inhibitor in the presence of 50 $\mu$g/mL DNase. After two centrifugation steps (100 g, 10 sec; 200 g, 5 min), resuspended cells were plated at a density of $2 \times 10^5$ cells/well onto poly-L-lysine-coated 96-well plates. After 24 h of incubation, cerebellar granule cells were incubated for 72 h with SHH (100 nM) and compounds at different concentrations. The cells were pulsed with [$^3$H]thymidine (25 $\mu$Ci/plate) 12 h before the end of the culture period. Treated plates were frozen 4 h at −20°C and then rapidly thawed at 37°C. Finally, cells were harvested onto filters (GF/C) using an automated cell harvester (PerkinElmer Life Sciences). The amount of incorporated radioactivity was quantified with a TopCount microplate scintillation counter (PerkinElmer Life Sciences). In pharmacological evaluations, stimulation induced by SHH at 100 nM was defined as 100 %, while baseline values (0% stimulation) were defined by the SHH-induced signal in the presence of a maximally active concentration of LDE-225.

## Topical treatment on depilated mice

### Depilation

Experiments were carried out using female C57BL6/NCrl mice (Charles River, L'Arbresle, France), aged 7 weeks on arrival (time at which the hair follicles are in telogen phase) (Muller-Rover et al. 2001). For depilation, mice were anesthetized (3 L/min oxygen, 3–4% isoflurane [Isovet, Primacal Healtcare UK Ltd.]) in an induction box and maintained under anesthesia by mask (2.5% isoflurane; 1.5 L/min). The back of the mice was depilated with

melted wax (Aries, Carros, France). Mice were thereafter housed individually for 5 days.

### Topical treatment

Preliminary studies for treatment optimization were conducted with LDE-225 and GDC-0449. Treatment duration was fixed to 8 h leading to the most pronounced inhibitions of Gli1 and Ptch1 gene expression (data not shown). Compounds were evaluated at different concentrations in two different vehicles: propylene glycol 60% (v/v)/DMSO 40% (v/v), annotated as PG60/D40, and propylene glycol 70% (v/v)/DMSO 20% (v/v)/EtOH 10% (v/v), annotated as PG70/D20/E10. For experiments, each treatment group included five mice. The control group was treated with the appropriate vehicle depending on the study. Compounds were extemporaneously dissolved in the appropriate vehicle at different concentrations (0.125–2% [w/v] depending on drug solubility). At day 5 post-depilation, 30 $\mu$L of the preparation was applied on the depilated back of the anesthetized mice and spread on all the depilated skin area (about 3 $cm^2$) with a micropipette tip. Mice were kept under anesthesia for 10 min to allow solution drying and to avoid grooming.

### Sampling

Exactly 8 h after treatment, mice were anesthetized and retro-orbital blood was sampled in a 5 $\mu$L heparin-aliquoted tube (Heparine Choay-5000 U/mL, Sanofi-Aventis, Paris, France). Mice were euthanized by cervical dislocation and the treated area was systematically rinsed twice with sterile gauze soaked in the appropriate vehicle before skin punches were sampled (6 mm diameter, Kruuse, Denmark).

## Quantification of Gli1 and Ptch1 gene expression by qPCR in skin biopsies

The punch of the skin was put in a lysis tube (Bertin Technologies, Montigny-le-Bretonneux, France) containing 850 $\mu$L of lysis buffer from the RNeasy Mini kit (Qiagen, Courtaboeuf, France) containing 1% of $\beta$-mercaptoethanol and homogenized with the Fastprep device (MP Biomedicals, Illkirch, France), flash-frozen in liquid nitrogen and stored at −80°C until use. Total RNA was automatically extracted in a QIAcube (Qiagen) with a RNeasy Mini kit (Qiagen). The integrity of the RNA was checked and its amount per sample quantified in a Bioanalyser Station (2100 Bioanalyser, Agilent, Les Ulis, France). First-strand cDNA was synthesized from an equal quantity of 500 ng of total RNA for each sample following the QuantiTect Reverse Transcription Kit protocol (Qiagen). Quantitative PCR were performed in a CFX96 thermocycler (Thermal Cycler, Biorad, Marnes-la-Coquette, France) in 96-well microtiter plates (Biorad, France) using the SsoFast EvaGreen Supermix (Biorad, France) as PCR mix. Primer sequences are given separately in the Supporting Information. Results were reported as relative expression using the comparative $2^{\Delta\Delta Ct}$ method normalized by the mean of two housekeeping genes: ribosomal protein PO (RPLPO) (GenBank: NM_007475) and cyclophilin (GenBank: NM_008907) in comparison to controls. RPLPO and cyclophilin were previously selected among six housekeeping genes as being the most stable genes between all conditions using Normfinder software (Andersen et al. 2004). Results (mean of at least five animals) are expressed as relative expression of Gli1 and Ptch1 mRNA versus vehicle-treated group (normalized to 1). Statistical significance was determined using an unpaired *t* test with o$P < 0.05$; *$P < 0.001$; #$P < 0.0001$.

## Quantitative determination of compound concentration in plasma samples and skin homogenates

The punch of the skin was put in a lysis tube (Bertin Technologies, France) containing 500 $\mu$L of water and homogenized with the Fastprep device (MP Biomedicals, Illkirch, France). The plasma samples or skin homogenates were processed using acetonitrile (AcN) precipitation and analyzed by HPLC-MS/MS (Supplementary Materials and Methods).

## Animal handling

Animals were handled and cared for in accordance with the Guide for the Care and Use of Laboratory Animals (Institute of Laboratory Animal Resources on Life Sciences, U.S. National Research Council, 2011) and the European Directive 2010/63/EU, and the protocols were carried out in compliance with French regulations and the local ethical committee guidelines for animal research, in an AAALAC International accredited facility (compare Supplementary Materials and Methods, for further details).

### Data analysis

All data are expressed as mean ± SEM. Isotherms were analyzed by nonlinear regression, using Prism software (GraphPad Software, La Jolla, CA, USA) to yield $IC_{50}$ values.

### Drugs

Compound sources are given in the Supplementary Material and Methods.

## Results

### Determination of G-protein activation in CHO cells by [$^{35}$S]GTP$\gamma$S binding

SMO-mediated G-protein activation was assessed in a [$^{35}$S]GTP$\gamma$S binding assay (Riobo et al. 2006; Shen et al. 2013) using a CHO cell line stably expressing the human SMO receptor isoform. The reference SMO agonist purmorphamine activated [$^{35}$S]GTP$\gamma$S incorporation in these cells, while the reference antagonist cyclopamine massively decreased basal [$^{35}$S]GTP$\gamma$S beyond basal levels (Fig. S1). Cyclopamine thus acted as an inverse agonist at the G-protein level, inhibiting constitutively active SMO (Riobo et al. 2006; Shen et al. 2013). Cyclopamine was defined as reference inverse agonist and included in each experiment (10 $\mu$M). Surprisingly, there was also a slight decrease of basal activity by another SMO agonist, SAG (Chen et al. 2002), which thus seems to act as a protean agonist at SMO (Fig. S1).

In the pharmacological comparison, all tested SMO antagonists yielded reductions in SMO constitutive activity (Table 1 and Fig. 1). Inhibitor $pIC_{50}$ values of the compounds were comprised between 8.06 (MRT-83) and 6.08 (CUR-61414). In terms of efficacy, most antagonists decreased basal signaling similar to cyclopamine and can thus be considered as equally efficacious inverse agonists. The notable exceptions are PF-5274857 and the antifungal itraconazole (Table 1). It should be noted that inhibition concentration–response curves of most compounds appeared biphasic and yielded slopes that were less than unity, indicating the possible implication of a two-site process (Fig. 1). This was however not observed for IPI-926 (Fig. 1), cyclopamine, CUR-61414, itraconazole and PF-5274857 (not shown).

In an additional set of experiments, we examined the impact of the SMO D473H point mutation that renders SMO insensitive to vismodegib (GDC-0449) binding, thus inducing acquired resistance to treatment with this drug (Metcalfe and de Sauvage 2011). In membrane preparations from CHO cells transiently transfected with the SMO D473H plasmid, cyclopamine induced a decrease in basal [$^{35}$S]GTP$\gamma$S binding, similar to the observations with wild-type (wt) SMO. However, the antagonist had lower potency at the D473H mutant (Table 1). As expected, GDC-0449 nearly completely lost its inverse agonist activity at SMO D473H, and some other compounds were severely affected by the D473H mutation, namely LDE-225 and PF-5274857 (Table 1). On the other hand, there was virtually no reduction in potency for CUR-61414, IPI-926, LEQ-506, and TAK-441.

SMO M2 is an oncogenic SMO variant that was identified in tumor samples of patients with BCC (Xie et al. 1998). SMO M2 carries the amino acid substitution

**Table 1.** Activity of SMO inhibitors in different in vitro assays.

| SMO wt inhibition | [$^3$H]Thymidine incorporation CGNP cells | GLI1 mRNA qPCR DAOY cells | [$^{35}$S]GTP$\gamma$S binding SMO wt | | [$^{35}$S]GTP$\gamma$S binding SMO D473H | | [$^{35}$S]GTP$\gamma$S binding SMO M2 | |
|---|---|---|---|---|---|---|---|---|
| | | | $pIC_{50}$ | $E_{max}$ | $pIC_{50}$ | $E_{max}$ | $pIC_{50}$ | $E_{max}$ |
| BMS-833923 | 8.53 ± 0.08 | 8.36 ± 0.19 | 6.76 ± 0.10 | −105.4 ± 2.5 | 6.43 ± 0.14 | −116.8 ± 1.6 | 6.39 ± 0.21 | −116.2 ± 16.4 |
| CUR-61414 | 7.52 ± 0.16 | <5.69 ± 0.34[1] | 6.08 ± 0.10 | −85.1 ± 6.3 | 6.04 ± 0.17 | −49.5 ± 8.9 | | |
| Cyclopamine | 6.32 ± 0.17 | 7.16 ± 0.27 | 7.20 ± 0.02 | −99.2 ± 2.1 | 6.28 ± 0.14 | −106.8 ± 1.8 | 6.45 ± 0.23 | −106.7 ± 3.5 |
| GDC-0449 | 8.01 ± 0.17 | 7.48 ± 0.11 | 7.57 ± 0.11 | −104.8 ± 2.3 | 4.62 ± 0.16 | −99.0 ± 11.8 | 6.32 ± 0.23 | −158.5 ± 22.9 |
| IPI-926 | 7.88 ± 0.19 | 7.93 ± 0.05 | 7.33 ± 0.09 | −105.3 ± 2.5 | 7.32 ± 0.03 | −114.1 ± 2.5 | 7.60 ± 0.08 | −97.9 ± 12.3 |
| Itraconazole | 6.76 ± 0.12 | 6.94 ± 0.07 | 6.27 ± 0.10 | −63.1 ± 2.4 | na | na | | |
| LY-2940680 | 8.12 ± 0.14 | 8.26 ± 0.08 | 6.53 ± 0.10 | −106.5 ± 1.8 | 6.22 ± 0.24 | −109.5 ± 12.3 | 5.75 ± 0.13 | −104.8 ± 18.9 |
| MRT-83 | 7.80 ± 0.03 | 8.35 ± 0.18 | 8.06 ± 0.18 | −88.6 ± 7.9 | 7.31 ± 0.11 | −115.1 ± 5.3 | | |
| LDE225 | 8.14 ± 0.08 | 7.96 ± 0.15 | 7.58 ± 0.04 | −105.6 ± 0.5 | 6.24 ± 0.06 | −103.7 ± 4.9 | 7.04 ± 0.11 | −143.6 ± 9.5 |
| LEQ-506 | 8.87 ± 0.18 | 9.13 ± 0.08 | 7.52 ± 0.05 | −104.3 ± 0.6 | 7.36 ± 0.20 | −112.7 ± 2.7 | 6.80 ± 0.11 | −111.5 ± 5.1 |
| PF-04449913 | 8.01 ± 0.08 | 8.35 ± 0.17 | 7.46 ± 0.09 | −103.8 ± 2.5 | 6.99 ± 0.19 | −118.3 ± 1.7 | 6.64 ± 0.10 | −130.3 ± 1.5 |
| PF-5274857 | 8.34 ± 0.09 | 7.97 ± 0.11 | 7.61 ± 0.14 | −60.4 ± 10.0 | 6.10 ± 0.19 | −76.3 ± 10.3 | | |
| TAK-441 | 8.15 ± 0.24 | 8.48 ± 0.18 | 6.81 ± 0.09 | −93.9 ± 5.9 | 6.79 ± 0.04 | −111.5 ± 6.3 | 5.87 ± 0.12 | −143.3 ± 13.3 |

Compounds were tested in rat CGNP cell proliferation experiments, in a GLI1 mRNA quantification assay performed with DAOY cells and in [$^{35}$S]GTP$\gamma$S incorporation tests using SMO-CHO cell membranes expressing recombinant wild-type (wt) SMO, SMO D473H or SMO M2. Data show inhibitor potencies (expressed as $pIC_{50}$) of the indicated compounds in all assays and efficacies ($E_{max}$) for [$^{35}$S]GTP$\gamma$S incorporation. The negative $E_{max}$ values indicate a decrease versus baseline, that is, an inverse agonist effect. na, not active.

[1]The activity of CUR-61414 was too weak to be quantified in four of six experiments. The $pIC_{50}$ given for this compound therefore indicates the average activity in the remaining two tests, but the actual potency can be considered weaker than this value.

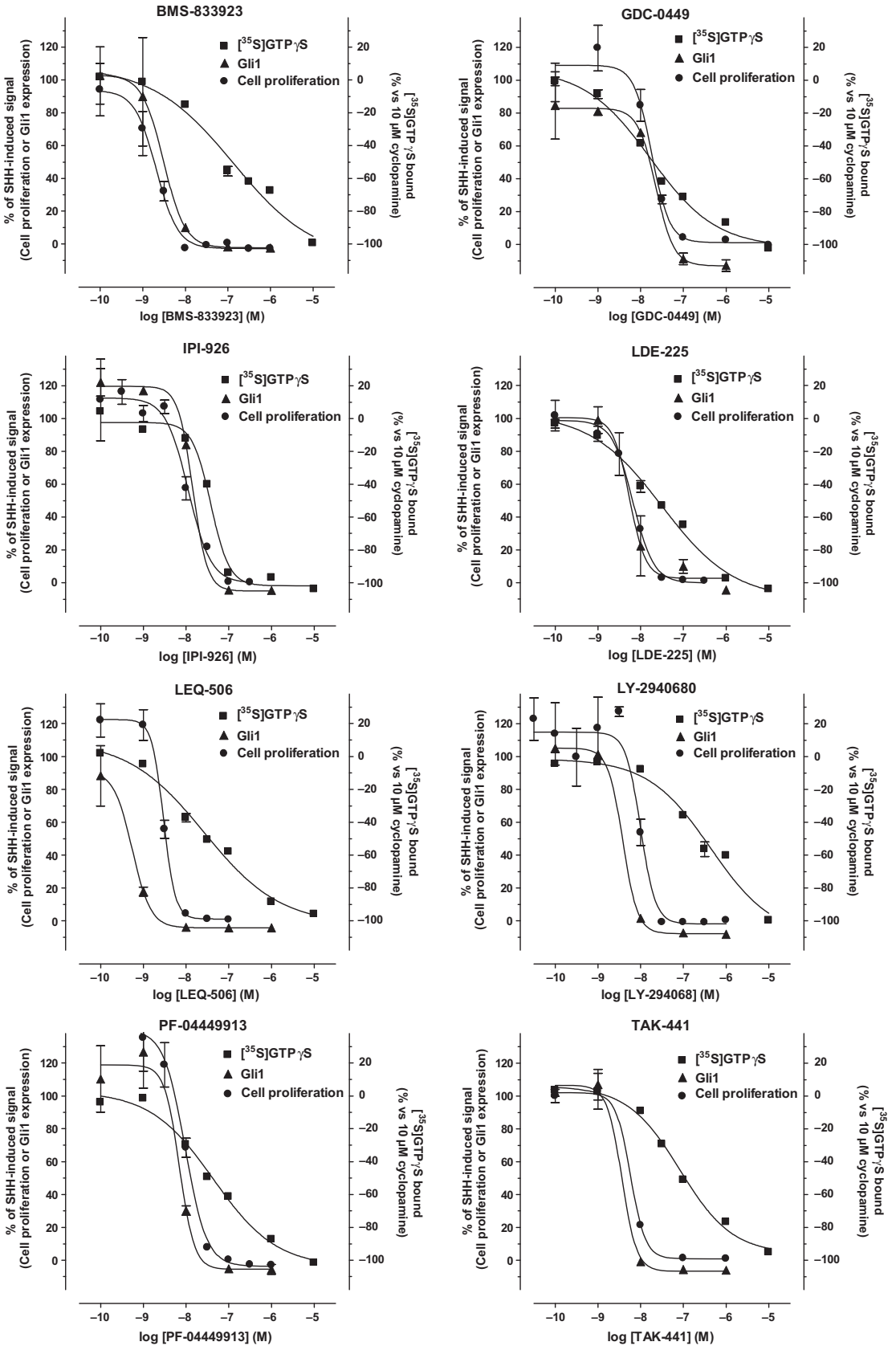

**Figure 1.** Comparison of eight selected smoothened antagonists in three in vitro assays for smoothened activity. Figures show concentration–response data of the indicated compounds in a [$^{35}$S]GTP$\gamma$S incorporation assay using SMO-CHO cell membranes (squares, [$^{35}$S]GTP$\gamma$S), a GLI1 mRNA quantification test using DAOY cells (triangles, GLI1), and rat CGNP cell proliferation experiments (circles, cell proliferation). All figures show representative duplicate or quadruplicate (CGNP cell proliferation) experimental determinations, each repeated at least three times. Data were fitted by nonlinear regression, using GraphPad Prism software. Please note the different scaling for inverse agonist activity ([$^{35}$S]GTP$\gamma$S binding, right *y*-axis) and antagonism against SHH-induced effects (left *y*-axis, both other tests). The average $pIC_{50}$ data of all compounds tested are given in Table 1.

W535L which prevents inhibition by PTCH, thereby inducing constitutive signaling activity (Murone et al. 1999). In [$^{35}$S]GTP$\gamma$S binding experiments with transiently transfected SMO M2, cyclopamine behaved as inverse agonist, but it had lower potency than at wt receptors and induced a lesser decrease of the basal signal when compared to experiments with transiently transfected wt SMO or SMO D473H (data not shown). The rather small and, moreover, variable decrease of the baseline signal was somewhat limiting for pharmacological experiments (due to small signal-to-noise ratio), and only a restricted set of clinically developed compounds was therefore tested with SMO M2. All these antagonists, like cyclopamine, behaved as inverse agonists for SMO M2 constitutive signaling (Table 1). Most compounds, similar to cyclopamine, were far less potent for inhibition of SMO M2 than for wt, with the exception of BMS-833923 and LDE-225 that exhibited only a slightly weaker $pIC_{50}$ and of IPI-926, which seemed even more potent at SMO M2.

## CGNP cell proliferation assay

The second pharmacological test employed to classify the activity of smoothened antagonists was a proliferation assay quantifying [$^{3}$H]thymidine incorporation in a rat cerebellar granule neuron precursor (CGNP) cellular model. Consistent with previous results (Wechsler-Reya and Scott 1999; Charytoniuk et al. 2002; Roudaut et al. 2011), SHH induced a concentration-dependent increase of proliferation in the assay. This effect was mimicked by the application of the SMO agonist, SAG (data not shown). The proliferation induced by SHH at 100 nM, which was the first maximally active dose of SHH (basal signal: 763 $\pm$ 94 dpms, SHH 100 nM: 17754 $\pm$ 3656 dpms), was near-completely reversed by application of the SMO inhibitor LDE-225. LDE-225 was included in each assay and used for normalization of pharmacological data (inhibition by LDE set to 100%). When diverse SMO inhibitors were evaluated in this assay, all compounds were similarly efficacious as LDE-225 for the inhibition of SHH-induced proliferation (see examples in Fig. 1). With the exception of the plant alkaloid cyclopamine and the antifungal itraconazole, SMO inhibitors displayed $IC_{50}$ values between 1 nM and 30 nM ($pIC_{50}$ between 7.5 and 9; Table 1). As a general trend, potencies in the proliferation assay were increased when compared to [$^{35}$S]GTP$\gamma$S binding, with as much as about 50-fold higher potencies in the case of BMS-833923 and LY-2940680 (Table 1 and Fig. 1). In a notable contrast, cyclopamine was not only the least potent compound tested, it also lost potency with respect to the membrane-based [$^{35}$S]GTP$\gamma$S assay (by a factor of 8, Table 1).

## GLI1 mRNA stimulation in DAOY cells

Compounds were further evaluated for their propensity to inhibit SHH-induced GLI1 mRNA stimulation in DAOY cells. These cells of human origin (derived from medulloblastoma) express the relevant machinery for HH-mediated signal transduction via SMO to GLI1 (Bar et al. 2007). DAOY cells therefore serve as a convenient model for the pharmacological examination of the HH pathway endogenously expressed in a disease-related cellular background. In the DAOY model, SHH consistently induced GLI1 mRNA, a biomarker of pathway activity (Scales and de Sauvage 2009). Cells were therefore routinely stimulated with SHH at a fixed concentration of 50 nM (which was also used as 100% reference) to determine inhibitor activity. All tested SMO antagonists completely inhibited the SHH-induced GLI1 induction in this model (Table 1). The $pIC_{50}$ values of most compounds for GLI1 mRNA inhibition were comprised between 7.5 and 9.1 (Table 1). Lesser potency was noted for itraconazole ($pIC_{50}$ 6.9) and CUR-61414 ($pIC_{50}$ 5.7).

## Assay comparison

When comparing the pharmacological outcome of the different in vitro tests, we observed large differences between the [$^{35}$S]GTP$\gamma$S assay on one hand and the DAOY GLI transcription as well as the CGNP cell test on the other (Table 1 and Fig. S2A). Indeed, inhibitor potencies were essentially in a similar range for the two latter assays (Table 1 and Fig. S2B). The striking exception of CUR-61414 (Table 1) may be explained by the loss of potency at the human SMO isoform that has been reported for this compound (Tang et al. 2011). An impact of the rat/human species difference can neither be excluded for other compounds with considerable

differences between the DAOY and the CGNP tests, such as MRT-83 and PF-5274857. However, there was still a much better correlation between the results of the proliferation and the GLI activation readouts than for each of them with [$^{35}$S]GTP$\gamma$S binding, even if both the DAOY cell line and transfected CHO cells implicate signaling via the human SMO isoform (Fig. S2A and B).

## Time course of Gli1 and Ptch1 expression in skin after depilation

The HH pathway plays a critical role for the regulation of growth and morphogenesis of hair follicles in adult skin (Oro and Scott 1998; Dlugosz 1999; Wang et al. 2000; Callahan and Oro 2001; Oro and Higgins 2003). During hair growth (anagen phase), there is a strong induction of HH target gene expression (such as Gli1 and Ptch1), a process that can be experimentally induced by the depilation of mouse skin (Paladini et al. 2005; Tang et al. 2011). This was confirmed in our experimental conditions by a comparison of Gli1 and Ptch1 gene expression in mouse skin at different times after depilation with an increase of both biomarkers that was rather stable from 4 to 7 days postdepilation (Fig. S3). The observed increase in Gli1 mRNA also translated into a higher level of the corresponding protein, as evidenced by immunohistochemistry in skin sections at 4 h and 5 days after depilation (Fig. S4). Surprisingly, there was no clear evidence for differential PTCH1 expression between these two postdepilation conditions (Fig. S4), probably indicating rapid turnover of this protein (Kawamura et al. 2008). Both biomarkers were therefore evaluated at the mRNA level at 5 days postdepilation as an indicator of HH pathway activity for further studies.

## Comparison of SMO antagonists after an 8-h treatment with a unique topical application

In preliminary experiments, we determined a vehicle that was appropriate for comparison of all compounds under the same conditions, at a concentration of 2% w/v. For solubility concerns, we selected a mixture of dimethylsulfoxide (DMSO) 40% and propylene glycol (PG) 60%. Even in this vehicle with high dissolving efficiency, the upper limit of solubility of LY-2940680 and CUR-61414 was only 1% and cyclopamine was insoluble. Another vehicle, with less DMSO and containing ethanol (PG70%, DMSO 20%, EtOH 10%), was subsequently used for concentration–response studies of a series of compounds (see below). Both vehicles showed no significant impact on the basal expression of Gli1 and Ptch1 genes as compared to non-treated skin (Fig. S5).

In pharmacological tests (Fig. 2A), LDE-225 exhibited an inhibition of 50–60% on Gli1 and Ptch1 mRNA and was systematically used as positive control. Although CUR-61414 and BMS-833923 were devoid of activity in this model, MRT-83 only slightly inhibited Ptch1 mRNA without any impact on Gli1. GDC-0449 and PF-04449913 decreased both biomarkers by about 40%. IPI-926 exhibited responses similar to LDE-225, decreasing Gli1 and Ptch1 mRNA by 50-60%. PF-527857, TAK-441, LY-2940680, and LEQ-506 were the most efficacious compounds by consistently decreasing Gli1 mRNA by about 70–80%. Interestingly, these latter compounds showed a tendency to preferentially inhibit Gli1 rather than Ptch1 mRNA.

When the distribution of compounds in plasma and skin was determined in parallel to biomarker quantifications, there were significant differences depending on the SMO antagonists used (Fig. 2B). In skin, the concentration of compounds ranged from 10 to 275 ng/mg and from 21 to 14,626 ng/mL in plasma. There was yet no obvious correlation between the activity of the compounds on Gli1 and Ptch1 repression and their concentrations in the skin and/or in plasma (compare Fig. 2A and B). Strikingly, the most efficacious compounds (LY-2940680 and LEQ-506) were found in low quantities both in skin (10 and 31 ng/mg, respectively) and in plasma (607 and 1874 ng/ml, respectively).

## Dose–effect of SMO antagonists after an 8-h treatment with a single topical application

The SMO antagonists showing a significant inhibition on Gli1 mRNA in the first part of the study were further tested in a dose-dependent manner (ranging from 0.125% to 2%, depending on the drug). We also reduced the DMSO concentration to 20% and we introduced 10% ethanol in the vehicle as this latter agent, largely used in topical formulations, was supposed to conceivably modify the activity of SMO antagonists. Unfortunately, the weakly soluble compound LY-2940680 formed a precipitate in the presence of ethanol at low concentrations and was therefore not further tested in PG70/D20/E10.

In pharmacological evaluations using this vehicle, almost all molecules tested at 2% exhibited a slightly better inhibition of the biomarkers (especially for Gli1 mRNA) compared to the vehicle PG60/D40 (compare Figs 2A and 3A). The only exception was PF-04449913 that was inactive. While GDC-0449, LDE-225, IPI-926 and PF-5274857 at 2% displayed a similar efficacy of inhibition (60–70%) for both biomarkers, their potencies were quite different. GDC-0449 lost its inhibitory activity at 1% whereas LDE-225 and IPI-926 were still (albeit

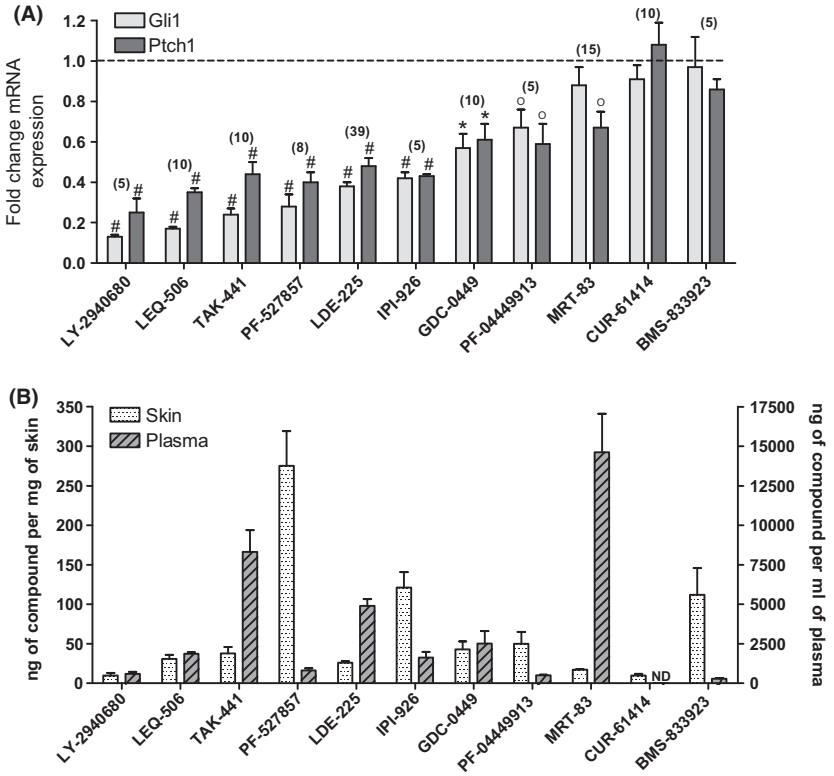


**Figure 2.** Assessment of compound activity in skin and quantification of their concentration in skin and plasma. Five days postdepilation, all compounds were tested for 8 h using a single topical application at 2% (w/v) except for LY-2940680 and CUR-61414 at 1% (w/v). (A) qPCR results on Gli1 and Ptch1 mRNA: the mean value of the control group treated with vehicle alone (propylene glycol 60%/DMSO 40%) was set to 1 (dashed line); bars represent the mean ± SEM of relative expression for each group. Number of animals is shown at the top of each bar. Statistical significance: o$P < 0.05$; *$P < 0.001$; #$P < 0.0001$. (B) Mean ± SEM of compound concentrations in skin biopsies (left axis) and corresponding plasma (right axis) determined by HPLC-MS/MS. ND, non detectable.

slightly less) active at 0.5 and 1%. PF-5274857 seemed quite potent because it was similarly active over the whole range of concentrations tested (0.5–2%). TAK-441 (at 2%) and LEQ-506 (at 1%) were the most efficacious compounds with an inhibition of 80–90% for Gli1 and of 60–70% for Ptch1. They also showed high potencies to inhibit the biomarkers, LEQ-506 being fourfold more potent than TAK-441 (see the similar efficacies of LEQ-506 at 0.25% when compared to TAK-411 at 1%, or LEQ-506 at 0.125% and TAK-411 at 0.5%, for example). Interestingly, there seemed to be a maximal inhibition level of about 70% for Ptch1 and of 90% for Gli1 under our experimental conditions.

The change of vehicle generally did not modify the partition of the compounds between plasma versus skin (compare Figs 2B and 3B). Not surprisingly, there was a higher accumulation of compounds in both skin and plasma with increasing application doses (with the notable exception of PF-527857 in plasma; Fig. 3B). Interestingly, however, the dose–response examination suggests that the skin presents different saturation levels depending on the SMO antagonists used.

## Discussion

The present study compares the pharmacological properties of SMO ligands in several early preclinical assays. In the first part of the study, the compounds were tested in three in vitro readouts, measuring [$^{35}$S]GTP$\gamma$S binding to transfected CHO cell membranes, proliferation of CGNP cells, and GLI transcriptional activity in DAOY cells. In the second part, we quantified markers of SMO activity in a depilated mouse model to evaluate the potential of the respective antagonists for a topical administration.

Data from the in vitro studies represent a basic pharmacological comparison of the diverse SMO inhibitors. While all three assays discriminate compounds with respect to their potency, it should be noted that the results of the CGNP proliferation and the DAOY/qPCR tests are much more consistent with each other than both

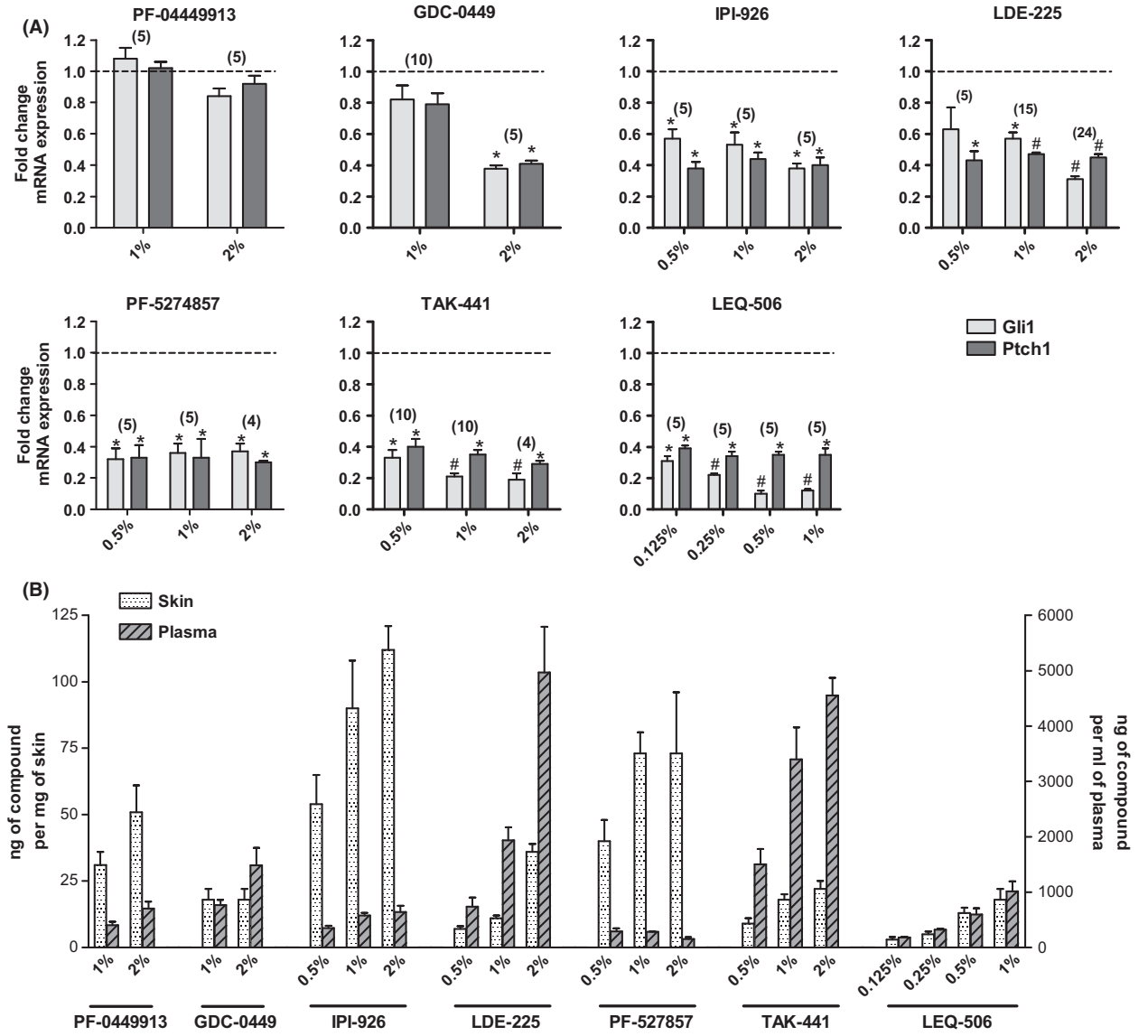


**Figure 3.** Assessment of compound dose–effect in skin and quantification of their concentration in skin and plasma. Five days postdepilation, all compounds were tested for 8 h using a single topical application. (A) qPCR on Gli1 and Ptch1 mRNA: the mean value of the control group treated with vehicle alone (propylene glycol 70%/DMSO 20%/ethanol 10%) was set to 1 (dashed line), bars represent the mean ± SEM of relative expression for each group. Number of animals is shown at the top of each bar. Statistical significance: $*P < 0.001$; $\#P < 0.0001$. (B) Compound concentrations in skin biopsies (left axis) and in corresponding plasma (right axis). Data represent mean ± SEM of compound concentrations determined by HPLC-MS/MS.

are with [$^{35}$S]GTP$\gamma$S binding. Indeed, in spite of the species differences between DAOY and CGNP cells, the range of compound potencies is fairly similar for the proliferation and the GLI1 mRNA assay, with the exception of CUR-61414. Moreover, the outcome of these tests seems in quite good accordance with previously published data (Tremblay et al. 2009; Mas and Altaba 2010; Hadden 2013). In fact, the disparity between the results for [$^{35}$S]GTP$\gamma$S binding and the other readouts was quite surprising, and several explanations seem possible. In contrast to the cellular assays, [$^{35}$S]GTP$\gamma$S binding is based on overexpression of recombinant SMO and the use of membrane preparations. Moreover, it measures constitutive SMO activity, that is, inhibitors are examined for their inverse agonist potencies. In contrast, both cellular assays are based on activation (or disinhibition) of SMO via SHH/PTCH. Beyond these considerations of assay conditions, it is also possible that the pharmacological

differences observed between the readouts are due to the fact that they imply different signaling mechanisms. Indeed, a large panel of canonical and noncanonical SMO-dependent pathways has been described which display some notable differences with respect to SMO inhibitor pharmacology (Ruat et al. 2014; Teperino et al. 2014). While an exhaustive discussion of these data is not possible here, they suggest at least the possibility that different tests might be complementary regarding to SMO signaling in different cellular contexts.

A particular point concerning the [$^{35}$S]GTP$\gamma$S assay is the observation of a biphasic pattern for most compounds, thus suggesting the existence of two different inhibition mechanisms with distinct potencies. While this putative two-site inhibition was not further investigated in our study, it is noteworthy that a biphasic behavior was not manifest for cyclopamine and its analog, IPI-926, as well as for itraconazole, PF-5274857 and CUR-61414. The latter three compounds did not appear as fully efficacious SMO inhibitors in the [$^{35}$S]GTP$\gamma$S assay, and it is tempting to speculate that this is the case because they do not engage both inhibitory processes that seem to exist. The case is different for cyclopamine and IPI-926, which seem fully active inverse agonists. Interestingly, however, these two compounds have been reported to be mechanistically different from vismodegib (GDC-0449) and other SMO antagonists in the context of a recently postulated two-step SMO activation process (Rohatgi et al. 2009); this concept implies that SMO activation first requires the transport of cytoplasmic SMO to the primary cilium of the cell, followed by a second activation step that converts the receptor into its final active conformation. While most SMO antagonists act on both these steps, cyclopamine and IPI-926 do not prevent the translocation to the cilium, but stabilize an inactive SMO conformation therein (Wang et al. 2012; Peluso et al. 2014). Thus, it seems possible that a single-conformation inhibition by cyclopamine and IPI-926 is manifest in the [$^{35}$S]GTP$\gamma$S readout, even if the implication of a transport process seems unlikely in the membrane-based assay.

The relative convenience of the [$^{35}$S]GTP$\gamma$S test prompted us to examine the pharmacological impact of SMO mutations, exemplified by the frequently discussed D473H (conferring vismodegib resistance to SMO) and W535L (constitutively active "SMO M2") single amino acid substitutions. These assays show that both mutations have a very different impact on inhibitory potency as a function of the antagonist tested. We thus support the notion that diverse antagonists may present a differential potential to act on particular oncogenic SMO isoforms.

The in vivo assay employed in the second part of the study more specifically addresses the topical efficacy of SMO antagonists. While there is currently no topical SMO antagonist treatment for superficial BCC in humans, dermal administration could allow a suppression of BCC or at least a reduction of their size before surgery, minimizing cosmetic impact. Moreover, topical treatment might restrict side effects when compared to systemic drug exposition. Indeed, topical administration allows a very local and limited application (surface/volume), if an appropriate vehicle (cream) can be determined. The depilated mouse model used is not directly related to BCC, but it has been shown to be a predictive pharmacodynamic readout of HH pathway activation in skin (Skvara et al. 2011; Tang et al. 2011) and thus constitutes a BCC-relevant model insofar as the vast majority of BCCs exhibits overactivation of the HH pathway (Johnson et al. 1996; Xie et al. 1998).

The readout of HH pathway activity in our model is based on Gli1 and Ptch1 gene expression. Autocontrolled Gli1 mRNA expression has already been shown to represent a relevant biomarker in depilated mouse skin in a similar model (Skvara et al. 2011; Tang et al. 2011). We confirm these observations and extend them to Ptch1, which is equally under control of Gli1 (Kasper et al. 2006).

To our knowledge, this is the first study that compares the topical activity of a large series of SMO antagonists. Overall, our approach clearly characterizes all molecules by their profiles of efficacy and potency. Most of the molecules tested herein have already demonstrated a certain efficacy in preclinical models of BCC and medulloblastoma. Even though PF-0449913 and BMS-833923 are currently in clinical development, they are ineffective on Gli1 and Ptch1 biomarkers in our model, suggesting that certain orally effective drugs may exhibit poor efficacy after topical application. Even GDC-0449 (vismodegib), which was the first marketed SMO antagonist with consistent efficacy for oral treatment of advanced stage BCC (Tang et al. 2012), promoted only an intermediate efficacy and weak potency for topical HH pathway inhibition.

Two compounds of our selection have been previously investigated for topical application on patients in small clinical trials. While LDE-225 showed efficacy for topical treatment of BCC (Skvara et al. 2011), CUR-61414 did not present any clinical activity in patients with superficial or nodular BCC, and neither did it decrease Gli1 mRNA (Tang et al. 2011). Both these compounds have also been tested on depilated mice, albeit with very different treatment schedules when compared to our protocol. LDE-225 (at 1%) was applied for 14 consecutive days, promoting an almost complete inhibition of Gli1 transcripts in mouse skin (Skvara et al. 2011). In our study, a single application of LDE-225 was already sufficient for significant inhibition of Gli1 and Ptch1 expression after

8 h. CUR-61414 was found to induce an 80% Gli1 inhibition after topical treatment with a 2% solution twice a day for 3 days (Tang et al. 2011). Thus, the lack of activity of this compound in our test is likely due to the stringency of our experimental conditions. In fact, it is likely that the activity of the lesser efficient molecules in our test could be generally improved by increasing the duration of treatments and the frequency of applications. However, given the accordance with clinical data described above, our experimental conditions chosen to allow a rapid discrimination of SMO antagonists in a topical set up might represent an effective model to predict and classify SMO antagonist efficacies.

One concern for SMO antagonists is their potentially weak safety margin as reported in several clinical trials, leading for instance to the high degree of discontinuation of vismodegib treatment via oral route (Sekulic et al. 2012). The partition between blood and skin might therefore represent an additional criterion to classify SMO antagonists for their development as a topical drug. Indeed, among the most active compounds, LY-2940680 and LEQ-506 showed a quite interesting distribution with weak plasma exposure in comparison to TAK-441 and LDE-225. An important factor to be taken into account in this context is doubtlessly the vehicle used for compound solubilization, which has to be adapted to each drug with respect to its physicochemical properties. Further studies with other vehicles are surely warranted as they might improve the pharmacodynamic properties of SMO antagonists.

In summary, the data presented constitute the first extensive pharmacological comparison of SMO inhibitors in diverse early preclinical tests. While the data of the in vitro assays determine SMO inhibitor potencies that constitute a common basis for a broad range of applications, the depilated mouse model more specifically addresses the suitability of the respective inhibitors for a topical application route.

## Acknowledgements

We thank Loïc Cerf from Fluofarma (Pessac, France) for his contribution to the ImmunoHistoChemistry experiments on mouse skin sections and helpful discussions.

## Author Contributions

Lauressergues, Heusler, Rauly-Lestienne, Lestienne, De Vries, Degryse, Dumoulin, and Cussac participated in the research design. Lauressergues, Lestienne, Tourette, Ailhaud, Tardif, Troulier, Cathala, Denais-Lalièves, and Calmettes conducted experiments. Troulier contributed new reagents or analytic tools. Lauressergues, Heusler, Rauly-Lestienne, Lestienne, Tourette, Ailhaud, Tardif, Troulier, Cathala, and Cussac performed data analysis. Lauressergues, Heusler, Rauly-Lestienne, Lestienne, De Vries, and Cussac wrote or contributed to the writing of the manuscript.

## Disclosure

All authors were full-time employees at the Pierre Fabre Research Institute at the time of the study.

## References

Amakye D, Jagani Z, Dorsch M (2013). Unraveling the therapeutic potential of the Hedgehog pathway in cancer. Nat Med 19: 1410–1422.

Andersen CL, Jensen JL, Orntoft TF (2004). Normalization of real-time quantitative reverse transcription-PCR data: a model-based variance estimation approach to identify genes suited for normalization, applied to bladder and colon cancer data sets. Cancer Res 64: 5245–5250.

Bar EE, Chaudhry A, Farah MH, Eberhart CG (2007). Hedgehog signaling promotes medulloblastoma survival via Bc/II. Am J Pathol 170: 347–355.

Callahan CA, Oro AE (2001). Monstrous attempts at adnexogenesis: regulating hair follicle progenitors through Sonic hedgehog signaling. Curr Opin Genet Dev 11: 541–546.

Charytoniuk D, Porcel B, Rodriguez GJ, Faure H, Ruat M, Traiffort E (2002). Sonic Hedgehog signalling in the developing and adult brain. J Physiol Paris 96: 9–16.

Chen JK, Taipale J, Young KE, Maiti T, Beachy PA (2002). Small molecule modulation of Smoothened activity. Proc Natl Acad Sci USA 99: 14071–14076.

Dlugosz A (1999). The Hedgehog and the hair follicle: a growing relationship. J Clin Invest 104: 851–853.

Dreier J, Dummer R, Felderer L, Nageli M, Gobbi S, Kunstfeld R (2014). Emerging drugs and combination strategies for basal cell carcinoma. Expert Opin Emerg Drugs 19: 353–365.

Hadden MK (2013). Hedgehog pathway inhibitors: a patent review (2009–present). Expert Opin Ther Pat 23: 345–361.

Johnson RL, Rothman AL, Xie J, Goodrich LV, Bare JW, Bonifas JM, et al. (1996). Human homolog of patched, a candidate gene for the basal cell nevus syndrome. Science 272: 1668–1671.

Kasper M, Regl G, Frischauf AM, Aberger F (2006). GLI transcription factors: Mediators of oncogenic Hedgehog signalling. Eur J Cancer 42: 437–445.

Kawamura S, Hervold K, Ramirez-Weber FA, Kornberg TB (2008). Two Patched Protein Subtypes and a Conserved Domain of Group I Proteins That Regulates Turnover*. J Biol Chem 283: 30964–30969.

Lin TL, Matsui W (2012). Hedgehog pathway as a drug target: smoothened inhibitors in development. Onco Targets Ther 5: 47–58.

Mas C, Altaba A (2010). Small molecule modulation of HH-GLI signaling: current leads, trials and tribulations. Biochem Pharmacol 80: 712–723.

Metcalfe C, de Sauvage FJ (2011). Hedgehog fights back: mechanisms of acquired resistance against Smoothened antagonists. Cancer Res 71: 5057–5061.

Muller-Rover S, Handjiski B, van der Veen C, Eichmuller S, Foitzik K, McKay IA, et al. (2001). A comprehensive guide for the accurate classification of murine hair follicles in distinct hair cycle stages. J Invest Dermatol 117: 3–15.

Murone M, Rosenthal A, de Sauvage FJ (1999). Hedgehog signal transduction: from flies to vertebrates. Exp Cell Res 253: 25–33.

Ng JM, Curran T (2011). The Hedgehog's tale: developing strategies for targeting cancer. Nat Rev Cancer 11: 493–501.

Oro AE, Higgins K (2003). Hair cycle regulation of Hedgehog signal reception. Dev Biol 255: 238–248.

Oro AE, Scott MP (1998). Splitting hairs: dissecting roles of signaling systems in epidermal development. Cell 95: 575–578.

Paladini RD, Saleh J, Qian C, Xu GX, Rubin LL (2005). Modulation of hair growth with small molecule agonists of the hedgehog signaling pathway. J Invest Dermatol 125: 638–646.

Peluso MO, Campbell VT, Harari JA, Tibbitts TT, Proctor JL, Whitebread N, et al. (2014). Impact of the Smoothened inhibitor, IPI-926, on smoothened ciliary localization and Hedgehog pathway activity. PLoS ONE 9: e90534.

Peukert S, Miller-Moslin K (2010). Small-molecule inhibitors of the hedgehog signaling pathway as cancer therapeutics. ChemMedChem 5: 500–512.

Pons S, Trejo JL, Martinez-Morales JR, Marti E (2001). Vitronectin regulates Sonic hedgehog activity during cerebellum development through CREB phosphorylation. Development 128: 1481–1492.

Riobo NA, Saucy B, Dilizio C, Manning DR (2006). Activation of heterotrimeric G proteins by Smoothened. Proc Natl Acad Sci USA 103: 12607–12612.

Rodon J, Tawbi HA, Thomas AL, Stoller RG, Turtschi CP, Baselga J, et al. (2014). A phase I, multicenter, open-label, first-in-human, dose-escalation study of the oral smoothened inhibitor Sonidegib (LDE225) in patients with advanced solid tumors. Clin Cancer Res 20: 1900–1909.

Rohatgi R, Milenkovic L, Corcoran RB, Scott MP (2009). Hedgehog signal transduction by Smoothened: pharmacologic evidence for a 2-step activation process. Proc Natl Acad Sci USA 106: 3196–3201.

Roudaut H, Traiffort E, Gorojankina T, Vincent L, Faure H, Schoenfelder A, et al. (2011). Identification and mechanism of action of the acylguanidine MRT-83, a novel potent Smoothened antagonist. Mol Pharmacol 79: 453–460.

Ruat M, Hoch L, Faure H, Rognan D (2014). Targeting of Smoothened for therapeutic gain. Trends Pharmacol Sci 35: 237–246.

Ruch JM, Kim EJ (2013). Hedgehog signaling pathway and cancer therapeutics: progress to date. Drugs 73: 613–623.

Scales SJ, de Sauvage FJ (2009). Mechanisms of Hedgehog pathway activation in cancer and implications for therapy. Trends Pharmacol Sci 30: 303–312.

Sekulic A, Migden MR, Oro AE, Dirix L, Lewis KD, Hainsworth JD, et al. (2012). Efficacy and safety of vismodegib in advanced basal-cell carcinoma. N Engl J Med 366: 2171–2179.

Shen F, Cheng L, Douglas AE, Riobo NA, Manning DR (2013). Smoothened is a fully competent activator of the heterotrimeric G protein G(i). Mol Pharmacol 83: 691–697.

Siu LL, Papadopoulos K, Alberts SR, Kirchoff-Ross R, Vakkalagadda B, Lang L, et al. (2010). A first-in-human, phase I study of an oral hedgehog (HH) pathway antagonist, BMS-833923 (XL139), in subjects with advanced or metastatic solid tumors. ASCO Meeting Abstracts 28: 2501.

Skvara H, Kalthoff F, Meingassner JG, Wolff-Winiski B, Aschauer H, Kelleher JF, et al. (2011). Topical treatment of Basal cell carcinomas in nevoid Basal cell carcinoma syndrome with a smoothened inhibitor. J Invest Dermatol 131: 1735–1744.

Tang T, Tang JY, Li D, Reich M, Callahan CA, Fu L, et al. (2011). Targeting superficial or nodular Basal cell carcinoma with topically formulated small molecule inhibitor of smoothened. Clin Cancer Res 17: 3378–3387.

Tang JY, Mackay-Wiggan JM, Aszterbaum M, Yauch RL, Lindgren J, Chang K, et al. (2012). Inhibiting the hedgehog pathway in patients with the basal-cell nevus syndrome. N Engl J Med 366: 2180–2188.

Tas S, Avci O (2004). Rapid clearance of psoriatic skin lesions induced by topical cyclopamine. A preliminary proof of concept study. Dermatology 209: 126–131.

Teperino R, Aberger F, Esterbauer H, Riobo N, Pospisilik JA (2014). Canonical and non-canonical Hedgehog signalling and the control of metabolism. Semin Cell Dev Biol 33C: 81–92.

Tremblay MR, Nesler M, Weatherhead R, Castro AC (2009). Recent patents for Hedgehog pathway inhibitors for the treatment of malignancy. Expert Opin Ther Pat 19: 1039–1056.

Vandesompele J, De Preter K, Pattyn F, Poppe B, Van Roy N, De Paepe A, et al. (2002) Accurate normalization of real-time quantitative RT-PCR data by geometric averaging of multiple internal control genes. Genome Biol 3: RESEARCH0034.

Varjosalo M, Taipale J (2008). Hedgehog: functions and mechanisms. Genes Dev 22: 2454–2472.

Wang LC, Liu ZY, Gambardella L, Delacour A, Shapiro R, Yang J, et al. (2000). Conditional disruption of hedgehog

signaling pathway defines its critical role in hair development and regeneration. J Invest Dermatol 114: 901–908.

Wang Y, Arvanites AC, Davidow L, Blanchard J, Lam K, Yoo JW, et al. (2012). Selective identification of hedgehog pathway antagonists by direct analysis of smoothened ciliary translocation. ACS Chem Biol 7: 1040–1048.

Wechsler-Reya RJ, Scott MP (1999). Control of neuronal precursor proliferation in the cerebellum by Sonic Hedgehog. Neuron 22: 103–114.

Xie J, Murone M, Luoh SM, Ryan A, Gu Q, Zhang C, et al. (1998). Activating Smoothened mutations in sporadic basal-cell carcinoma. Nature 391: 90–92.

Xie J, Bartels CM, Barton SW, Gu D (2013). Targeting hedgehog signaling in cancer: research and clinical developments. Onco Targets Ther 6: 1425–1435.

## Supporting Information

Additional Supporting Information may be found in the online version of this article:

**Data S1.** Supplementary Materials and Methods
**Figure S1**. Reference ligands in [$^{35}$S]GTPγS binding.
**Figure S2**. Correlation of inhibitor potencies in vitro.
**Figure S3**. Time course of Gli1 and Ptch1 mRNA expression in mouse skin.
**Figure S4**. Expression profile of GLI1 and PTCH1 by immunohistochemistry.
**Figure S5**. Impact of vehicles on Gli1 and Ptch1 mRNA expression.